Europe PMC Funders Group
Author Manuscript
Science. Author manuscript; available in PMC 2019 January 08.

Published in final edited form as:
Science. 2014 October 17; 346(6207): 318–322. doi:10.1126/science.1254960.

Motor skill learning requires active central myelination

Ian A. McKenzie[#1], **David Ohayon**[#1], **Huiliang Li**[1], **Joana Paes de Faria**[1,†], **Ben Emery**[2], **Koujiro Tohyama**[3], and **William D. Richardson**[1,‡]

[1]The Wolfson Institute for Biomedical Research, University College London, Gower Street, London WC1E 6BT, UK

[2]Department of Anatomy and Neuroscience and the Florey Institute for Neuroscience and Mental Health, University of Melbourne, Melbourne, Victoria 3010, Australia

[3]The Center for Electron Microscopy and Bio-Imaging Research, Iwate Medical University, 19-1 Uchimuru, Morioka, Iwate 020-8505, Japan

[#] These authors contributed equally to this work.

Abstract

Myelin-forming oligodendrocytes (OLs) are formed continuously in the healthy adult brain. In this work, we study the function of these late-forming cells and the myelin they produce. Learning a new motor skill (such as juggling) alters the structure of the brain's white matter, which contains many OLs, suggesting that late-born OLs might contribute to motor learning. Consistent with this idea, we show that production of newly formed OLs is briefly accelerated in mice that learn a new skill (running on a "complex wheel" with irregularly spaced rungs). By genetically manipulating the transcription factor myelin regulatory factor in OL precursors, we blocked production of new OLs during adulthood without affecting preexisting OLs or myelin. This prevented the mice from mastering the complex wheel. Thus, generation of new OLs and myelin is important for learning motor skills.

Myelin is the spirally wrapped cell membrane that surrounds and insulates axons in the central and peripheral nervous systems (CNS and PNS, respectively). Myelin greatly increases the speed of electrical communication among neurons and, hence, the brain's computational power. CNS myelin is synthesized by oligodendrocytes (OLs), the majority of which develop in the first 6 postnatal weeks in rodents, from proliferating OL precursors [(OPs), also known as NG2 glia] (1, 2). However, many OPs persist in the adult mouse CNS (~5% of all neural cells) and continue to divide and differentiate into myelinating OLs throughout life (1–3). For example, nearly 30% of OLs in the 8-month-old corpus callosum are formed after 8 weeks of age (2). What is the function of adult-born OLs and myelin? Magnetic resonance imaging (MRI) has detected changes in the structure of white matter in people trained in complex sensorimotor tasks such as playing the piano, juggling, or abacus use (4–6). Analogous MRI changes are observed in rats during motor training (7). The histological basis of the MRI change is not known, but one possibility is that newly

[‡]**Corresponding author.** w.richardson@ucl.ac.uk.
[†]Present address: Instituto de Biologia Molecular e Celular, Rua do Campo Alegre 823, 4150-180 Porto, Portugal.

Europe PMC Funders Author Manuscripts
Europe PMC Funders Author Manuscripts

Europe PMC Funders Author Manuscripts

Europe PMC Funders Author Manuscripts

generated myelin is laid down preferentially in circuits that are engaged during motor learning. Here we show that active myelination during adulthood is required for motor skill learning and that motor learning increases OL production.

Preventing adult myelination by conditional deletion of myelin regulatory factor

Myelin regulatory factor (MyRF) is a transcription factor required in OLs to initiate and maintain their myelination program (8–10). It is not expressed in OPs, in other CNS cells, or in Schwann cells, which myelinate PNS axons. We have a mouse line that carries a "floxed" allele of *Myrf* (10). By breeding (see supplementary materials and methods), we obtained *Myrf*$^{(+/flox)}$ and *Myrf*$^{(flox/flox)}$ littermates on a *Pdgfra-CreER*^{T2}*: Rosa-YFP* background (2, 11); we refer to these as *P-Myrf*$^{(+/flox)}$ and *P-Myrf*$^{(flox/flox)}$, respectively. Administering tamoxifen induces Cre-mediated recombination, inactivating one or both alleles of *Myrf* in *Pdgfra*-expressing OPs while simultaneously labeling the OPs with yellow fluorescent protein (YFP) (see supplementary materials and methods). We refer to the tamoxifen-treated mice as *P-Myrf*$^{(+/-)}$ and *P-Myrf*$^{(-/-)}$. Recombination at the *Myrf* locus was confirmed by reverse transcription polymerase chain reaction (fig. S1).

We inactivated *Myrf* in OPs by tamoxifen administration on postnatal day 60 (P60) or P90. Subsequently, we identified YFP$^+$ OPs and newly differentiated YFP$^+$ OLs by triple-immunolabeling with anti-YFP, anti-Pdgfra (for OPs), and the CC1 monoclonal antibody (for OLs). In *P-Myrf*$^{(+/-)}$ mice, YFP$^+$,CC1$^+$,Pdgfra$^-$ OLs accumulated in the anterior corpus callosum (beneath the motor cortex) after the administration of tamoxifen (post-tamoxifen) (arrows in Fig. 1A). In *P-Myrf*$^{(-/-)}$ mice, production of YFP$^+$,CC1$^+$ OLs was decreased to ~10% of control (Fig. 1, A and B); at 1 month post-tamoxifen, we counted 301 ± 59 YFP$^+$,CC1$^+$ cells/mm^2 in 20-μm sections of *P-Myrf*$^{(+/-)}$ corpus callosum but only 33 ± 7 cells/mm^2 in *P-Myrf*$^{(-/-)}$ (means ± SEM; six fields of view in three sections of three mice of each genotype). There was a comparable reduction in other regions of the *P-Myrf*$^{(-/-)}$ brain, including the cerebral cortex, striatum, midbrain, and cerebellum. In the motor cortex, for example, we counted 123 ± 15 YFP$^+$,CC1$^+$ cells/mm^2 in *P-Myrf*$^{(+/-)}$ and 10 ± 3 cells/mm^2 in *P-Myrf*$^{(-/-)}$. There was no recovery of OL production over at least 3 months (Fig. 1B). Loss of newly formed OLs was confirmed visually using a different reporter line, *Tau-mGFP* (GFP, green fluorescent protein), that expresses a membrane-bound green fluorescent protein, revealing whole-cell morphology including the myelin sheaths (3, 12). One month post-tamoxifen, *P-Myrf*$^{(-/-)}$*:Tau-mGFP* corpus callosum was almost devoid of GFP-positive myelin sheaths, in contrast to their *Myrf*$^{(+/-)}$ littermates, which had many (Fig. 1C).

To quantify new OL production in *P-Myrf*$^{(-/-)}$ versus *P-Myrf*$^{(+/-)}$ mice, we administered 5-ethynyl-2′-deoxyuridine (EdU) to P60 mice for 1 week, after tamoxifen treatment. One month later, 5.7% ± 0.7% of CC1$^+$ OLs in *P-Myrf*$^{(+/-)}$ corpus callosum were positive for EdU (i.e., recently formed from cycling OPs), compared with only 0.20% ± 0.07% in *P-Myrf*$^{(-/-)}$ littermates (means ± SEM; six fields, >250 OLs per field in three sections of three mice of each genotype) (fig. S2). Therefore, *Myrf* was deleted in >90% of all OPs, whether or not they recombined the *Rosa-YFP* reporter. Over the same period, we detected no

Europe PMC Funders Author Manuscripts

Europe PMC Funders Author Manuscripts

significant changes in the number density of Pdgfra$^+$ OPs or CC1$^+$,YFP$^-$ (i.e., preexisting) OLs in *P-Myrf*$^{(-/-)}$ versus *P-Myrf*$^{(+/-)}$ corpus callosum (Fig. 1D). Therefore, our strategy prevents the formation of new OLs without affecting preexisting OLs.

Preventing new OL production does not trigger demyelination

Myelin histochemistry with Eriochrome cyanine (Life Technologies) showed that *P-Myrf*$^{(-/-)}$ mice had normal-appearing white matter (Fig. 2, A and B), indistinguishable from their *P-Myrf*$^{(+/-)}$ littermates (Fig. 2, C and D). In contrast, when *Myrf*$^{(flox/flox)}$ was deleted conditionally in both OLs and OPs using *Sox10-CreER*^{T2} mice [*S10-Myrf*$^{(-/-)}$] (see supplementary materials and methods and fig. S3), there was dramatic loss of myelin (Fig. 2, E and F). Electron microscopy (EM) revealed compact myelin sheaths in *P-Myrf*$^{(-/-)}$ mice (Fig. 2, G and H) that were indistinguishable from *P-Myrf*$^{(+/-)}$ controls (Fig. 2, I and J), whereas *S10-Myrf*$^{(-/-)}$ mice were severely demyelinated (Fig. 2, K and L). Phagocytic cells (macrophages or activated microglia) containing cell debris were observed by EM in *S10-Myrf*$^{(-/-)}$ corpus callosum (34 cells counted in four fields from two P90 mice 5 weeks post-tamoxifen; mean cell density ~220 cells/mm^2) (Fig. 2M); such cells were much less frequent in *P-Myrf*$^{(-/-)}$ (7 cells; ~44 cells/mm^2) or in *P-Myrf*$^{(+/-)}$ controls (10 cells; ~55 cells/mm^2). For comparison, the density of OPs in the healthy CNS is ~150 cells/mm^2. There was no evidence of inflammation or blood-brain barrier breakdown marked by invasion of immune cells (e.g., neutrophils or T cells), loss of tight junctions between endothelial cells, or retraction of astrocyte processes from blood vessels, even in the severely demyelinated *S10-Myrf*$^{(-/-)}$ brain.

Consistent with the myelin histology, *P-Myrf*$^{(-/-)}$ mice showed no outward signs of demyelination (e.g., tremors) and were indistinguishable from their *P-Myrf*$^{(+/-)}$ littermates on an accelerating rotarod, a test for motor coordination and balance (Fig. 2N). In contrast, *S10-Myrf*$^{(-/-)}$ mice developed severe tremors around 1 month posttamoxifen (movie S1), and their performance on the rotarod was seriously impaired (Fig. 2O), similar to when *Myrf* deletion was targeted to mature OLs using *Plp-CreER* (9).

The complex running wheel

We assessed motor learning ability using a running wheel with irregularly spaced rungs (“complex wheel”) (Fig. 3) (13, 14). Mice run on the wheel spontaneously and, when skilled, can run the equivalent of 5 to 7 km per night. When wildtype (WT) (C57B6/CBA hybrid) mice accustomed to a regular wheel with equally spaced rungs are switched to the complex wheel, they experience great difficulty at first but persevere and after about a week can run as fast on the complex wheel as they can on the regular wheel (movies S2 and S3). High-speed filming reveals that on the regular wheel mice adopt a symmetrical “running walk” with an eight-gap stride, out of phase by four gaps left to right (15) (Fig. 3A). They bring their hindpaws up to the rung immediately behind their forepaws. On the complex wheel, they break step, adopting an asymmetrical gait with six- to nine-gap strides out of phase by two to six gaps between sides. A critical adaptation is that the mice bring their hindpaws forward to grasp the same rung as their forepaws (Fig. 3, B to E). Thus, their hindpaws always find a rung, whatever the pattern of gaps. They also prefer rungs preceded

Europe PMC Funders Author Manuscripts

Europe PMC Funders Author Manuscripts

by a one- or two-rung gap (Fig. 3, B to D); presumably, they reach forward into a gap and "pull back" to grasp the nearest rung, a second adaptation that is transferable to other rung patterns. Therefore, mice do not memorize specific stepping patterns but develop general strategies for running on wheels with unequal gaps; mastering one rung pattern primes them to master a different pattern more easily (fig. S4).

Active myelination is required for motor skill learning

Learning to run on the complex wheel presumably engages motor control circuits in addition to those required for normal symmetrical gait, involving the basal ganglia, cerebellum, motor cortex, and connecting pathways including the corpus callosum, but independent of the hippocampus (16–18). We introduced *P-Myrf*$^{(-/-)}$ and *P-Myrf*$^{(+/-)}$ littermates (mixed C57B6/CBA/129 background, predominantly C57B6; see supplementary materials and methods) to the complex wheel 3 weeks after tamoxifen treatment beginning on P60 (four experiments) or P90 (one experiment) (Fig. 4, A and B). The P90 experiment is shown (Fig. 4, C to F). Both cohorts improved their performance during the first week on the complex wheel, but the daily average and maximum speeds attained by the *P-Myrf*$^{(-/-)}$ group were always less than their *P-Myrf*$^{(+/-)}$ siblings (Fig. 4, C and D). Time spent turning the wheel >1 m/min was the same for both genotypes, arguing against a difference in motivation (Fig. 4E). Individual performances varied widely, and there was substantial overlap between genotypes (Fig. 4F). Pooled data for all five experiments confirmed significant differences in the average speeds attained by *P-Myrf*$^{(-/-)}$ versus *P-Myrf*$^{(+/-)}$ animals (Fig. 4G), as well as their individual performances (Fig. 4H) [$P = 0.0063$, Kolgomorov-Smirnov (K-S) nonparametric test; $n = 32$ and 36 mice, respectively]. One-third (12 of 36) of *P-Myrf*$^{(+/-)}$ mice ran further in 1 week than the best-performing of their *P-Myrf*$^{(-/-)}$ counterparts (Fig. 4H). High-speed filming showed that *P-Myrf*$^{(-/-)}$ mice ran less rhythmically and sometimes appeared to propel the wheel with their rear ankle or lower leg rather than their hindpaw (movies S4 and S5). The average speeds of *P-Myrf*$^{(+/-)}$ mice (on the seventh day) had an approximately normal distribution ($P = 0.2$, K-S test), whereas the average speeds of *P-Myrf*$^{(-/-)}$ mice were bimodal and skewed toward lower speeds (different distributions, $P = 0.007$) (Fig. 4I), possibly reflecting multistage learning (Fig. 3). The maximum speed distribution of *P-Myrf*$^{(-/-)}$ mice was also shifted to lower speeds ($P < 0.0001$) (Fig. 4J). When retested 1 month later, the difference between *P-Myrf*$^{(-/-)}$ and *P-Myrf*$^{(+/-)}$ animals persisted (fig. S4). There were no significant differences between males and females (fig. S5).

Active myelination is not required to recall a prelearned skill

Despite the lack of a general locomotor defect on the rotarod, *Myrf* deletion could have caused some subtle neural or physical impairment unrelated to learning. To control for this, we introduced P60 *P-Myrf*$^{(flox/flox)}$ and *P-Myrf*$^{(+/flox)}$ littermates to the complex wheel before tamoxifen treatment (Fig. 4K). As expected, the two cohorts were indistinguishable before tamoxifen (Fig. 4L and fig. S6). We administered tamoxifen, housed the mice singly for 3 weeks without a wheel, and then reintroduced them to the complex wheel (Fig. 4K). Both *P-Myrf*$^{(-/-)}$ and *P-Myrf*$^{(+/-)}$ groups were immediately able to run at speed (Fig. 4L and fig. S6). We conclude that (i) *P-Myrf*$^{(-/-)}$ mice are inherently able to run at speed on the

Europe PMC Funders Author Manuscripts

Europe PMC Funders Author Manuscripts

complex wheel (i.e., they are physically capable) and (ii) myelin formation is not required to perform a prelearned skill.

Running stimulates OP proliferation and OL production

To relate motor learning to cell dynamics, we introduced P60 WT mice to the complex wheel while administering EdU via their drinking water, and we counted EdU^+ cells in the corpus callosum after various periods. At 4 days, there was a transient increase (~40%, $P = 0.006$, $n = 4$) in the fraction of $Pdgfra^+$ OPs that was EdU-labeled ("labeling index") in runners relative to control mice housed without a wheel, indicating that running had accelerated the G_1-to-S transition (Fig. 5A). This was followed 2 days later by a spike in the absolute number of $Pdgfra^+$ OPs as they completed the cell cycle (~40% increase, $P = 0.04$, $n = 3$) (Fig. 5B), then 5 days after that (11 days running) by an increase (~40%, $P = 0.003$, $n = 3$) in the number of EdU^+,$Pdgfra^-$ cells—a mixture of $CC1^+$ and $CC1^-$ OLs (Fig. 5C). At 11 days, almost all (94% ± 4%) EdU^+ cells were $Sox10^+$ OL lineage cells. After 3 weeks, there were many newly formed EdU^+,$CC1^+$ OLs in control animals housed without a wheel, as expected (2, 3), but a ~50% greater number of those cells in runners (Fig. 5D).

The transient increase in EdU labeling index was not observed a second time when the complex wheel was removed from the cage and reintroduced 1 week later (Fig. 5, E and F), suggesting that it was triggered by novel experience (e.g., learning), not exercise per se. OP division and differentiation was increased by running on the regular wheel (fig. S7) as well as the complex wheel, suggesting that the region of corpus callosum we examined is involved in skills common to both (e.g., grasping or general bilateral coordination).

The cellular events described above occurred on a similar time scale as the improvement in running performance and, together with our data from *Myrf* knockout mice, support an important role for newly formed OLs in motor skill acquisition. How might new myelinating cells contribute to skill learning? It is likely that new neuronal connections are formed, or existing connections strengthened, in response to repetitive firing of neural circuits that elicit a particular sequence of movements (18). The increased activity in these circuits might then stimulate myelination of their axons, or myelin remodeling, making the circuit more efficient. There might even be a reserve of preformed, parallel circuits in the brain, and motor training selects the best of these by stimulating myelination in the most active circuits. The fact that most axons in the mouse corpus callosum and cerebral cortex remain incompletely myelinated into adulthood could be consistent with this idea (19, 20). The existence of an activity-driven myelination mechanism has been postulated, based on the fact that OPs express various neurotransmitter receptors, form synapses with naked axons, and display transmembrane ion currents in response to action potentials in the axons that they contact (21–25). There is evidence that activity or experience can regulate OP division and differentiation in vivo [(26–32) and this paper] and also MRI evidence of structural changes in the white matter of individuals learning sensorimotor skills (4–7), undertaking working memory training (33), or learning a second language (34). We have now provided experimental evidence that OL genesis and myelin formation are important for motor learning and, therefore, are likely to contribute to the changes observed by MRI. Future

Europe PMC Funders Author Manuscripts

Europe PMC Funders Author Manuscripts

experiments can assess whether new myelinating cells are required for other types of learning as well.

Supplementary Material

Refer to Web version on PubMed Central for supplementary material.

Acknowledgments

We thank the staff of the Center for Electron Microscopy and Bio-Imaging Research, Iwate Medical University, and U. Dennehy and M. Grist (University College London) for technical help and our colleagues in the Wolfson Institute for Biomedical Research for encouragement and suggestions. W.D.R. thanks T. Richardson for stimulating discussions. The study was supported by the European Research Council (grant agreement 293544), the UK Medical Research Council, the Wellcome Trust, and Grants-in-Aid from the Japanese Ministry of Education, Culture, Sports, Science and Technology. W.D.R. and K.T. acknowledge an Invitation Fellowship from the Japan Society for Promotion of Science. I.M. was supported by a Royal Society USA/Canada Exchange Fellowship, J.P.d.F. by a fellowship from the Portuguese Fundação para a Ciência e a Tecnologia, and B.E. by a Career Development Fellowship from the Australian National Health and Medical Research Council. *Pdgfra-CreER^{T2}* and *Sox10-CreER^{T2}* mice can be obtained by request through www.e-lucid.com/ with a material transfer agreement. *Myrf(flox)* mice can be obtained from Jackson Laboratories, strain 010607. The supplementary materials include additional data.

References

1. Richardson WD, Young KM, Tripathi RB, McKenzie I. Neuron. 2011; 70:661–673. [PubMed: 21609823]
2. Rivers LE, et al. Nat Neurosci. 2008; 11:1392–1401. [PubMed: 18849983]
3. Young KM, et al. Neuron. 2013; 77:873–885. [PubMed: 23473318]
4. Bengtsson SL, et al. Nat Neurosci. 2005; 8:1148–1150. [PubMed: 16116456]
5. Scholz J, Klein MC, Behrens TE, Johansen-Berg H. Nat Neurosci. 2009; 12:1370–1371. [PubMed: 19820707]
6. Hu Y, et al. Hum Brain Mapp. 2011; 32:10–21. [PubMed: 20235096]
7. Sampaio-Baptista C, et al. J Neurosci. 2013; 33:19499–19503. [PubMed: 24336716]
8. Emery B, et al. Cell. 2009; 138:172–185. [PubMed: 19596243]
9. Koenning M, et al. J Neurosci. 2012; 32:12528–12542. [PubMed: 22956843]
10. Bujalka H, et al. PLOS Biol. 2013; 11
11. Srinivas S, et al. BMC Dev Biol. 2001; 1:4. [PubMed: 11299042]
12. Hippenmeyer S, et al. PLOS Biol. 2005; 3:e159. [PubMed: 15836427]
13. Liebetanz D, et al. Exp Neurol. 2007; 205:207–213. [PubMed: 17341420]
14. Hibbits N, Pannu R, Wu TJ, Armstrong RC. ASN Neuro. 2009; 1:153–164.
15. Hildebrand M. Bioscience. 1989; 39:766–775.
16. Grillner S. Neuron. 2006; 52:751–766. [PubMed: 17145498]
17. Schalomon PM, Wahlsten D. Brain Res Bull. 2002; 57:27–33. [PubMed: 11827734]
18. Milner B, Squire LR, Kandel ER. Neuron. 1998; 20:445–468. [PubMed: 9539121]
19. Sturrock RR. Neuropathol Appl Neurobiol. 1980; 6:415–420. [PubMed: 7453945]
20. Tomassy GS, et al. Science. 2014; 344:319–324. [PubMed: 24744380]
21. Bakiri Y, et al. Neuroscience. 2009; 158:266–274. [PubMed: 18314276]
22. Bergles DE, Jabs R, Steinhäuser C. Brain Res Rev. 2010; 63:130–137. [PubMed: 20018210]
23. Gallo V, Mangin JM, Kukley M, Dietrich D. J Physiol. 2008; 586:3767–3781. [PubMed: 18635642]
24. Maldonado PP, Vélez-Fort M, Angulo MC. J Anat. 2011; 219:8–17. [PubMed: 21352226]
25. Fields RD. Semin Cell Dev Biol. 2011; 22:214–219. [PubMed: 21320624]
26. Simon C, Götz M, Dimou L. Glia. 2011; 59:869–881. [PubMed: 21446038]

27. Gibson EM, et al. Science. 2014; 344
28. Barres BA, Raff MC. Nature. 1993; 361:258–260. [PubMed: 8093806]
29. Li Q, Brus-Ramer M, Martin JH, McDonald JW. Neurosci Lett. 2010; 479:128–133. [PubMed: 20493923]
30. Makinodan M, Rosen KM, Ito S, Corfas G. Science. 2012; 337:1357–1360. [PubMed: 22984073]
31. Mangin JM, Li P, Scafidi J, Gallo V. Nat Neurosci. 2012; 15:1192–1194. [PubMed: 22885848]
32. Wake H, Lee PR, Fields RD. Science. 2011; 333:1647–1651. [PubMed: 21817014]
33. Takeuchi H, et al. J Neurosci. 2010; 30:3297–3303. [PubMed: 20203189]
34. Schlegel AA, Rudelson JJ, Tse PU. J Cogn Neurosci. 2012; 24:1664–1670. [PubMed: 22571459]

Europe PMC Funders Author Manuscripts

Europe PMC Funders Author Manuscripts

Europe PMC Funders Author Manuscripts

Europe PMC Funders Author Manuscripts

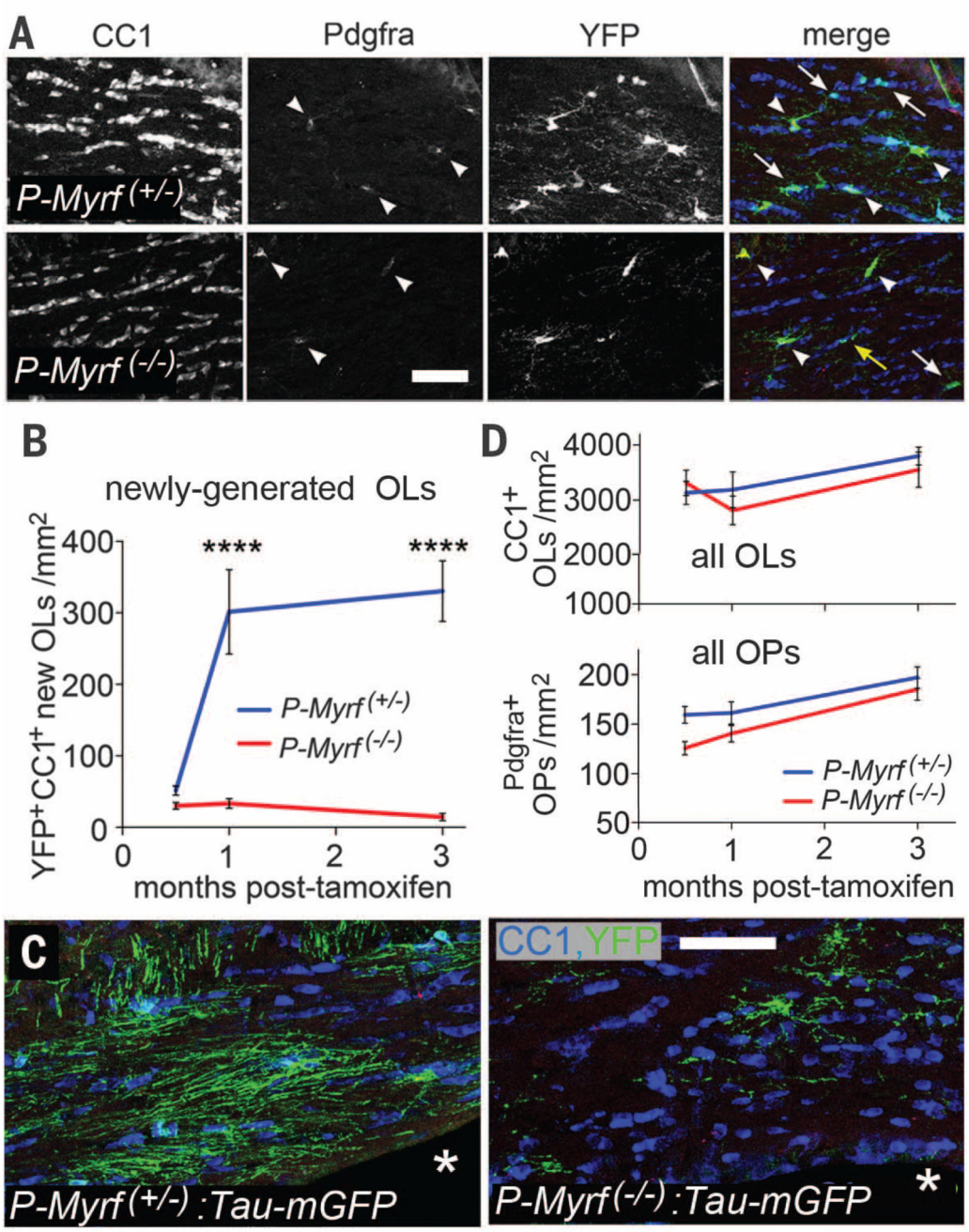

Fig. 1. Deleting *Myrf* in OPs prevents new myelination.

(**A**) Many YFP$^+$ (newly formed) cells accumulated 1 month after tamoxifen treatment in the *P-Myrf*$^{(+/-)}$ corpus callosum, including Pdgfra$^+$,CC1$^-$ OPs (arrowheads) and CC1$^+$, Pdgfra$^-$ OLs (arrows). In contrast, the *P-Myrf*$^{(-/-)}$ corpus callosum contained few YFP$^+$ cells, mainly Pdgfra$^+$ OPs. Some YFP$^+$,CC1$^+$ cells appeared fragmented, presumably because they are apoptotic (yellow arrow). (**B**) Numbers of YFP$^+$,CC1$^+$ OLs in the *P-Myrf*$^{(-/-)}$ versus *P-Myrf*$^{(+/-)}$ corpus callosum (****$P < 0.0001$). Error bars indicate SEM. (**C**) Very few GFP$^+$ (newly formed) myelin sheaths are present in the *P-Myrf*$^{(-/-)}$*:Tau-mGFP* corpus callosum 1

month post-tamoxifen relative to *P-Myrf*$^{(+/-)}$ siblings. Asterisk indicates third ventricle. (**D**) The number densities of Pdgfra^{+} OPs or CC1^{+},YFP^{-} (preexisting) OLs did not change between P60 and P150. Error bars indicate SEM. Scale bars: 50 μm, (A) and (C).

Europe PMC Funders Author Manuscripts

Europe PMC Funders Author Manuscripts

Europe PMC Funders Author Manuscripts

Europe PMC Funders Author Manuscripts

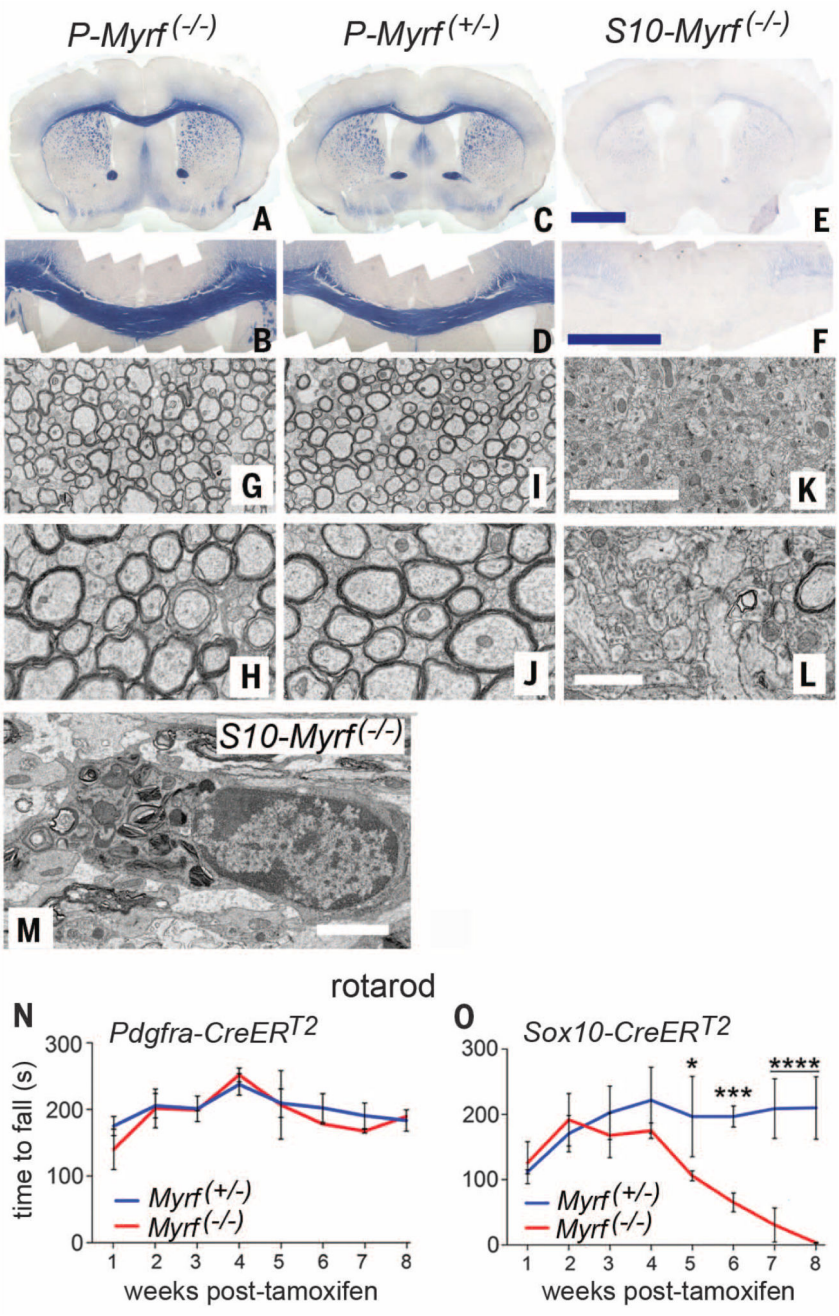

Fig. 2. Deleting *Myrf* in OPs does not trigger demyelination.

Tamoxifen was administered to P60 mice and, 5 weeks later, their brains were examined by Eri-C histochemistry (**A** to **F**) or electron microscopy (**G** to **M**). There was no visible loss of myelin in *P-Myrf*$^{(-/-)}$ [(A), (B), (G), and (H)] or *P-Myrf*$^{(+/-)}$ [(C), (D), (I), and (J)] brains, but there was marked demyelination in *S10-Myrf*$^{(-/-)}$ [(E), (F), (K), and (L)]. In *S10-Myrf*$^{(-/-)}$ white matter, phagocytic cells containing membrane debris were present (M). Performance on an accelerating rotarod was not impaired in *P-Myrf*$^{(-/-)}$ mice for at least 8 weeks post-tamoxifen compared with their *P-Myrf*$^{(+/-)}$ littermates (**N**),whereas *S10-*

Myrf$^{(-/-)}$ mice were seriously impaired after 4 to5 weeks (**O**). Error bars indicate SEM. *$P <$ 0.05; ***$P < 0.001$; ****$P < 0.0001$. Scale bars: 2 mm, (A), (C), and (E); 1 mm, (B), (D), and (F); 5 μm, (G), (I), and (K); 1 μm, (H), (J), and (L); and 2 μm (M).

Europe PMC Funders Author Manuscripts

Europe PMC Funders Author Manuscripts

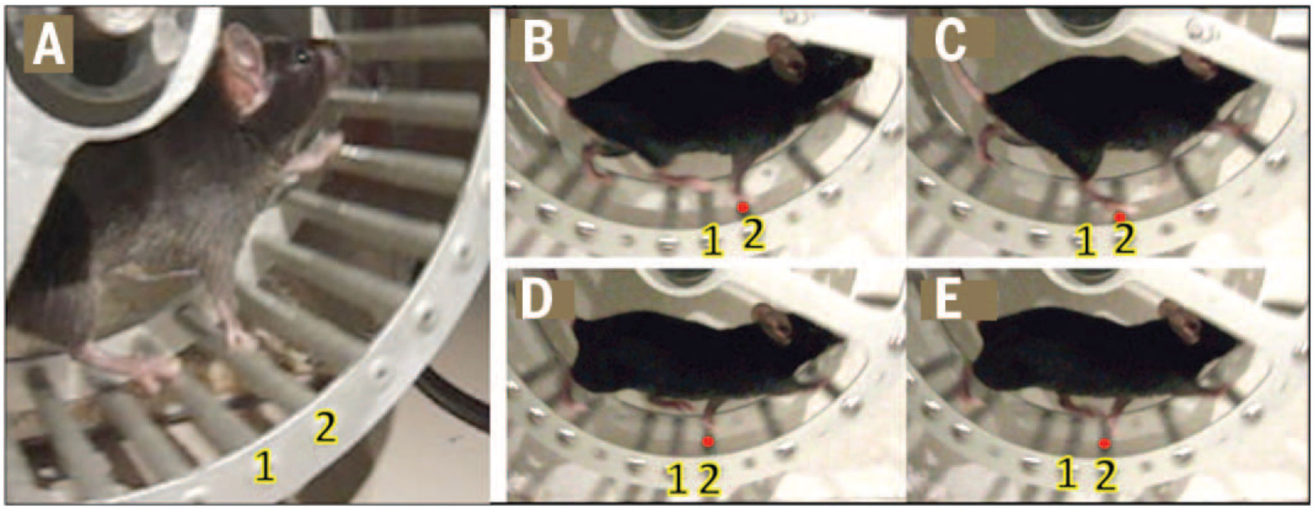

Fig. 3. Mice learn general strategies for coping with uneven rung spacing.

(**A**) On the regular running wheel, WT mice place fore- and hindpaws on consecutive rungs while reaching forward with the contralateral forepaw. (**B** to **E**) On the complex wheel, they grasp the same rung with fore- and hindpaws (red dots), selecting rungs preceded by a one- or two-rung gap [e.g., (B) and (D)]. These strategies are transferable to other rung patterns. (B) and (C) and (D) and (E) are consecutive video frames (240 frames/s).

Europe PMC Funders Author Manuscripts

Europe PMC Funders Author Manuscripts

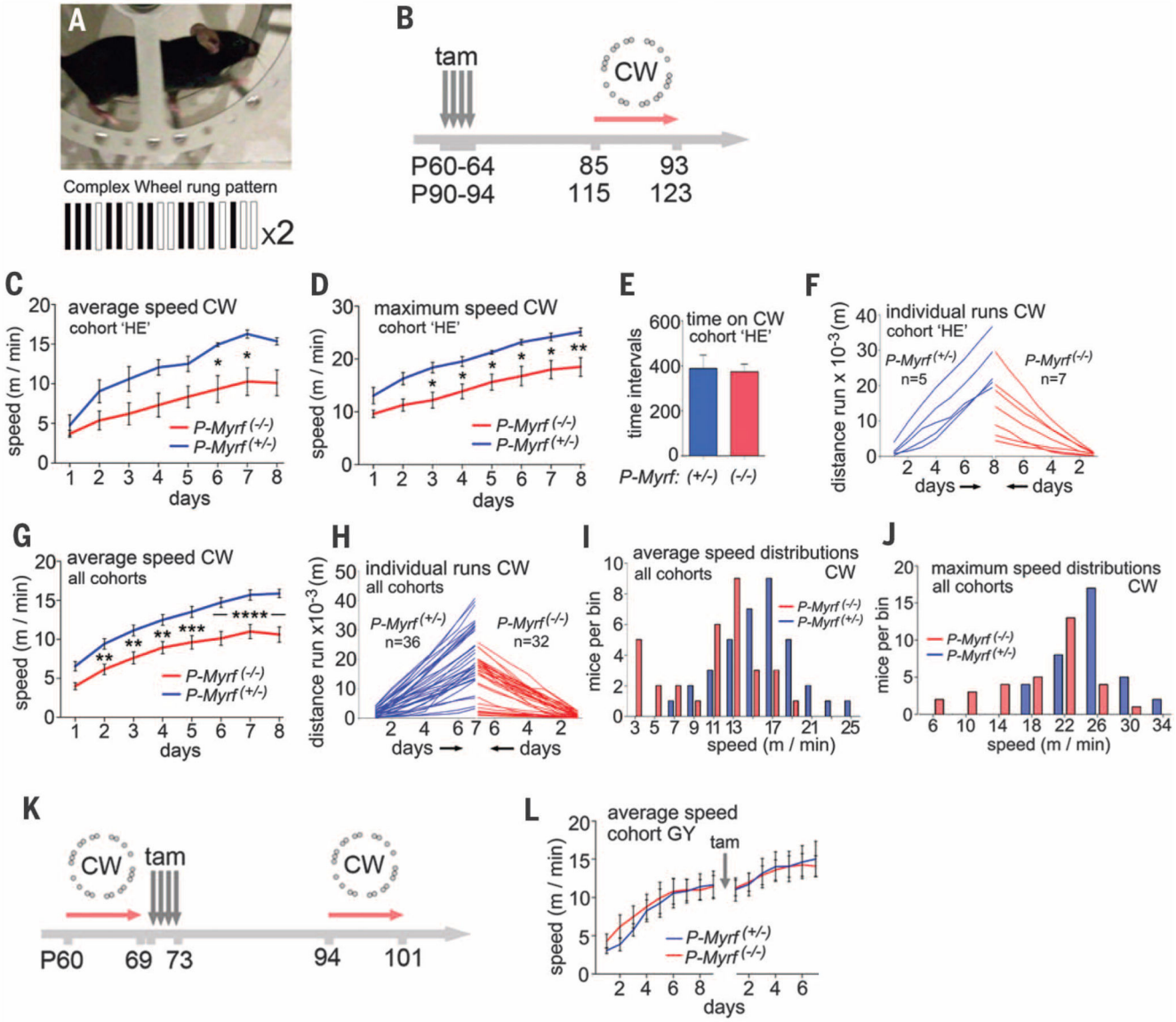

Fig. 4. Active CNS myelination is required for motor skill learning.

(**A**) The complex wheel pattern. (**B**) Experimental design. *P-Myrf*$^{(-/-)}$ and *P-Myrf*$^{(+/-)}$ mice were housed singly, and tamoxifen was administered from P60 or P90. Three weeks later, they were introduced to the complex wheel (CW). (**C** and **D**) On the wheel, *P-Myrf*$^{(-/-)}$ mice were impaired relative to *P-Myrf*$^{(+/-)}$ [tamoxifen on P90; means ± SEM (error bars), n = 7 and 5, respectively]. (**E**) Time on wheel at >1 m/min was not different between cohorts. Error bars denote SEM. (**F**) Individual performances, distance versus time. (**G** to **J**) Five pooled experiments confirm divergence between *P-Myrf*$^{(+/-)}$ and *P-Myrf*$^{(-/-)}$ mice [P = 0.0063 for accumulated distances, P = 0.0003 for average speeds; K-S test, n = 36 (20 males) and 32 (17 males), respectively]. Error bars in (G) denote SEM. (**K** and **L**) *P-Myrf*$^{(+/flox)}$ and *P-Myrf*$^{(flox/flox)}$ mice were introduced to the complex wheel before tamoxifen exposure and reintroduced 3 weeks after treatment. Both before and after, there

Europe PMC Funders Author Manuscripts
Europe PMC Funders Author Manuscripts

was no difference between cohorts ($n = 7$ and 8, respectively). Error bars in (L) denote SEM. $*P < 0.05$; $**P < 0.01$; $***P < 10^{-3}$; $****P < 10^{-4}$. Also see fig. S6.

Europe PMC Funders Author Manuscripts

Europe PMC Funders Author Manuscripts

Europe PMC Funders Author Manuscripts

Europe PMC Funders Author Manuscripts

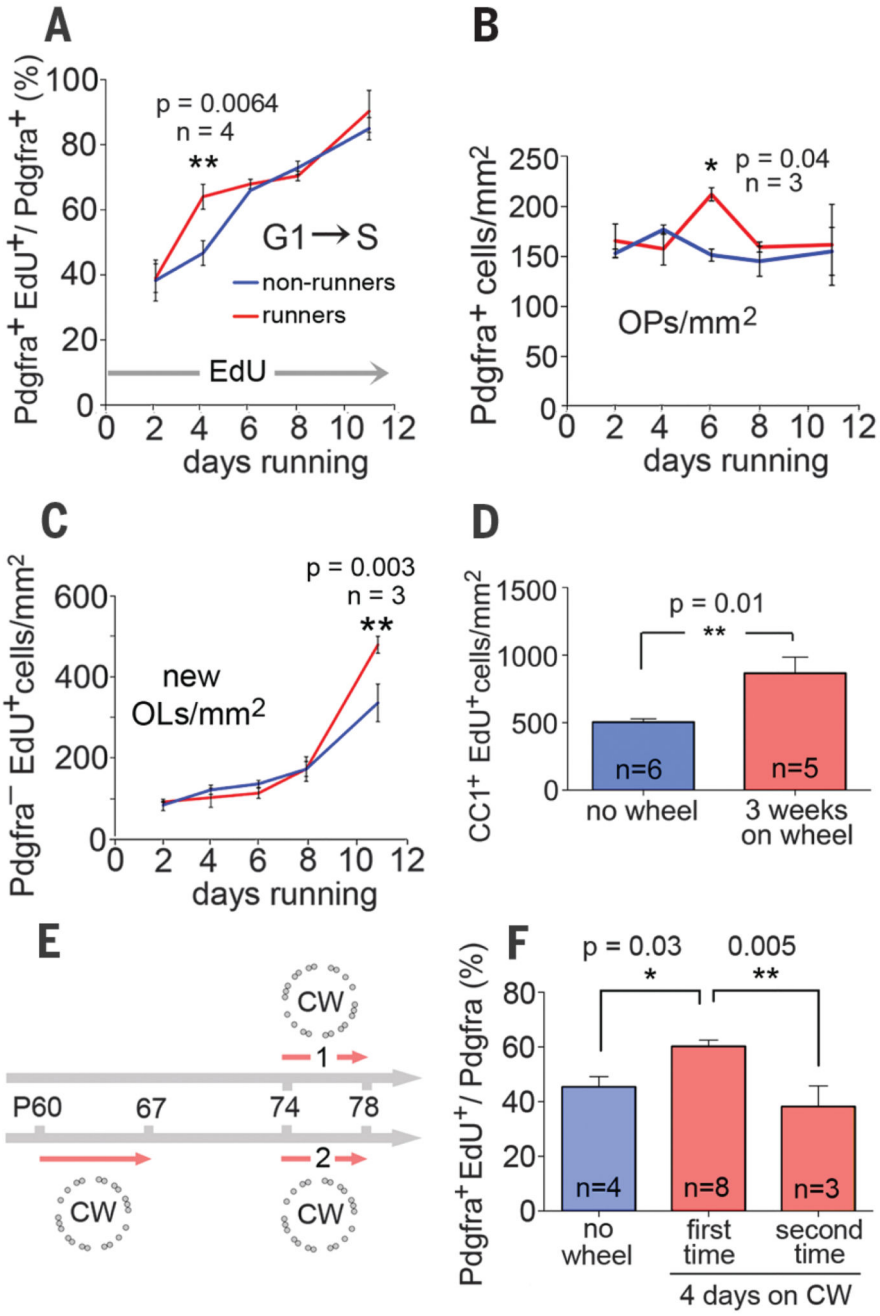

Fig. 5. Running stimulates OP proliferation and OL production.

Running on the complex wheel (CW) caused (**A**) a transient increase in the EdU labeling index of Pdgfra$^+$ OPs in the corpus callosum after 2 days, (**B**) an increase in the number density of OPs at 6 days, and (**C**) increased production of OLs (EdU$^+$,Pdgfra$^-$) by 11 days. The latter were a mixture of mature CC1$^+$ and immature CC1$^-$ OLs. The numbers of both cell types were greater in runners than nonrunners at 11 days, although individually the increases did not reach significance (P = 0.15 and 0.06, respectively). (**D**) After 3 weeks running, there were ~50% more EdU$^+$,CC1$^+$ OLs in runners than nonrunners. (**E**)

Experimental design. EdU was administered in the drinking water for 4 days during running, as indicated (arrows 1 and 2). (**F**) The EdU labeling index was increased by the first but not the second encounter with the wheel. Each data point represents multiple fields from at least three sections from three or more mice. Error bars in (A) to (D) and (F) represent SEM. Also see fig. S7.

Europe PMC Funders Author Manuscripts

Europe PMC Funders Author Manuscripts